

# Growth, domain dynamics and piezoelectric properties of some lead-free ferroelectric crystals

Guisheng Xu · Danfeng Yang · Kai Chen ·  
David A. Payne · James F. Carroll III

Received: 25 August 2007 / Accepted: 13 January 2009 / Published online: 28 January 2009  
© Springer Science + Business Media, LLC 2009

**Abstract** Lead-free solid solution crystals  $(\text{Na}, \text{Bi})\text{TiO}_3$ – $\text{BaTiO}_3$  [NBBT] and  $(\text{K}, \text{Na})\text{NbO}_3$ – $\text{LiNbO}_3$  [KNN–LN] have been grown by the Bridgman method. Their piezoelectric constant  $d_{33}$  reach 160 and 405 pC/N, respectively. Domain dynamics shown through in-situ observation using a polarizing microscopy in 0.94NBT-0.06BT crystals demonstrate that both of ferroelectric–antiferroelectric phase transition and antiferroelectric–paraelectric one take place in broad temperature ranges. 0.94NBT-0.06BT is more relaxor ferroelectric whereas 0.95KNN-0.05LN crystal is more normal ferroelectric. Moreover, it is found that the ferroelectric phase coexists with the paraelectric phase at the temperature much higher than their Curie temperature in both crystals. The low value of  $d_{33}$  may originate from the existence of an antiferroelectric tetragonal phase in a ferroelectric rhombohedral phase in NBBT crystals.

**Keywords** Lead-free piezoelectric crystals ·  
 $(\text{Na}, \text{Bi})\text{TiO}_3$ – $\text{BaTiO}_3$  ·  $(\text{K}, \text{Na})\text{NbO}_3$ – $\text{LiNbO}_3$  ·  
Phase transition

## 1 Introduction

From the viewpoint of sustainable development of the world society, the use of lead-based piezoelectric materials may be prohibited by law in the near future. More and more attention has been paid to lead-free piezoelectric materials in recent years. Among the researches on these materials, more attention was focused on lead-free piezoelectric ceramics and some exciting results have been published. For example, it was reported that textured alkaline niobate ceramics  $(\text{K}, \text{Na})\text{NbO}_3$ – $\text{LiTaO}_3$ – $\text{LiSbO}_3$  exhibited a piezoelectric constant  $d_{33}$  up to as high as 416 pC/N with Curie temperature  $T_c \sim 253^\circ\text{C}$  [1], and  $0.8(\text{Na}_{0.5}, \text{Bi}_{0.5})\text{TiO}_3$ – $0.2(\text{K}_{0.5}, \text{Bi}_{0.5})\text{TiO}_3$  ceramics near the Morphotropic Phase Boundary (MPB) of  $(\text{Na}_{0.5}, \text{Bi}_{0.5})\text{TiO}_3$ – $(\text{K}_{0.5}, \text{Bi}_{0.5})\text{TiO}_3$  solid solution system, which were prepared by the conventional technique, also showed  $d_{33}$  constant of 325 pC/N [2]. These novel lead-free ceramics have achieved piezoelectric properties almost as good as PZT ceramics'. Meanwhile, compared with lead-free piezoelectric ceramics, the researches on lead-free crystals were carried out insufficiently. Owing to the difficulties in the sintering density encountered in the fabrication of many lead-free ceramics, it is necessary to study other type lead-free materials, like lead-free crystals. Moreover, crystals may exhibit more excellent piezoelectric properties than their ceramics counterparts due to the crystallographic anisotropy and domain engineering, which has been found in the studies on relaxor-based ferroelectric single crystals  $\text{Pb}(\text{Zn}_{1/3}\text{Nb}_{2/3})\text{O}_3$ – $\text{PbTiO}_3$  (PZNT) and  $\text{Pb}(\text{Mg}_{1/3}\text{Nb}_{2/3})\text{O}_3$ – $\text{PbTiO}_3$  (PMNT)[3–5].

It was reported that small size  $0.945(\text{Na}_{0.5}\text{Bi}_{0.5})\text{TiO}_3$ – $0.055\text{BaTiO}_3$  crystals could exhibit  $d_{33}$  value up to 450 pC/

G. Xu (✉) · D. Yang · K. Chen  
R&D Center of Synthetic Crystals,  
Shanghai Institute of Ceramics, Chinese Academy of Sciences,  
Shanghai, China  
e-mail: gshxu@mail.sic.ac.cn

G. Xu · D. A. Payne · J. F. Carroll III  
Department of Materials Science and Engineering,  
University of Illinois at Urbana Champaign,  
Urbana, IL, USA

N on the (001) cuts [6] whereas alkaline niobate solid solution crystals were reported rarely. The properties and structures of large  $(\text{Na}_{0.5}\text{Bi}_{0.5})\text{TiO}_3\text{-BaTiO}_3$  (NBBT) crystals and alkaline niobate crystals are not clear. In this paper, some results of growth, domain dynamics and properties of lead-free piezoelectric crystals NBBT and  $(\text{K}_{0.5}\text{Na}_{0.5})\text{NbO}_3\text{-LiNbO}_3$  (KNN–LN) will be presented.

## 2 Experimental procedure

0.94NBT-0.06BT and 0.95KNN-0.05LN crystals near the MPB were prepared using a Bridgman technique, and the detailed growth process could refer to the papers [7, 8]. The obtained crystals were sliced to plates along (001) cuts. Polished samples with the thickness of 0.3–0.4 mm were used for optical observation. In-situ observation using the optical polarizing microscopy with hot stage was carried out to demonstrate the domain dynamics. The heating and cooling rate of 3°C/min was chosen for the observation. For electrical characterization, silver electrodes were used. The NBBT were poled at 4.0 kV/mm for 15 min at 170°C, and KNN–LN at 4.0 kV/mm for 30 min at 140°C. Their dielectric properties were measured using an Agilent 4294A precision impedance analyzer and piezoelectric constant  $d_{33}$  was measured with Berlincourttype quasistatic meter of ZJ-4A type.

## 3 Results and discussion

### 3.1 Growth results and electrical properties

0.94NBT-0.06BT crystal boules reached the size of  $\Phi 20 \times 110$  mm and their plates were yellowish and transparent. 0.95KNN-0.05LN crystals were milk white and semitransparent. XRD data indicate that both of them are of pure

perovskite structures, and 0.94NBT-0.06BT crystals are of rhombohedral phase and 0.95KNN-0.05LN of orthorhombic phase. Table 1 shows their dielectric and piezoelectric properties on the (001) cuts. The value of  $d_{33}$  constant (160 pC/N) of 0.94NBT-0.06BT crystals is lower than the reported 450 pC/N in reference [6] although it is slightly higher than their ceramics counterpart (125 pC/N) [9]. Meanwhile, it was also reported that 0.94NBT-0.06BT crystals did not show piezoelectricity at all [10]. Therefore, we think that the factors leading to the decrease of  $d_{33}$  constant of NBBT crystals may be complicated. On the other hand, 0.95KNN-0.05LN crystals show high  $d_{33}$  of 405 pC/N, which is almost the same as textured (K,Na)  $\text{NbO}_3\text{-LiTaO}_3\text{-LiSbO}_3$  ceramics [1].

Figures 1 and 2 show the temperature dependence of dielectric properties of NBBT and KNN–LN crystals respectively. It can be seen that 0.94NBT-0.06BT crystals have ferroelectric rhombohedral–antiferroelectric tetragonal phase transition at  $T_{rt} \sim 198^\circ\text{C}$  and antiferroelectric tetragonal–paraelectric cubic phase transition at  $T_c \sim 330^\circ\text{C}$ . Compared to 0.94NBT-0.06BT ceramics [13],  $T_{rt}$  and  $T_c$  go up for 0.94NBT-0.06BT crystals. The difference between crystals and ceramics may arise from their fabrication methods. Compositional segregation or compositional deviation from charged raw materials occurs during growth of these solid solution crystals [7]. On the other hand, it is found that the temperature of dielectric constant maximum drop with increasing frequency for the NBBT crystals, which was also observed in 0.94NBT-0.06BT and 0.92NBT-0.08BT ceramics [13]. This dielectric dispersion is different from that in such relaxor ferroelectrics as PMN and originates from anti-ferroelectric–paraelectric phase transition, instead of ferroelectric–paraelectric transition. 0.95KNN-0.05LN crystals have the ferroelectric orthorhombic–ferroelectric

**Table 1** Dielectric and piezoelectric properties of 0.94NBT-0.06BT and 0.95KNN-0.05LN crystals on (001) cuts in comparison with other fine lead-free materials.

Parameters	Single crystal			Ceramic	
	KNN–LN	NBBT	BNT-KNT70/30 <sup>a</sup>	KNN–LN <sup>b</sup>	Textured KNN <sup>c</sup>
$T_c$ (°C)	428	330	365	490	253
$d_{33}$ (pC/N)	405	160	160	314	416
$k_t, k_p$ (%)	$k_t$ 61	–	$k_t$ 49	$k_p$ 41	$k_p$ 61
Loss (%)	2.7	–	–	–	–

<sup>a</sup> Reference [11]

<sup>b</sup> Reference [12]

<sup>c</sup> Reference [1]

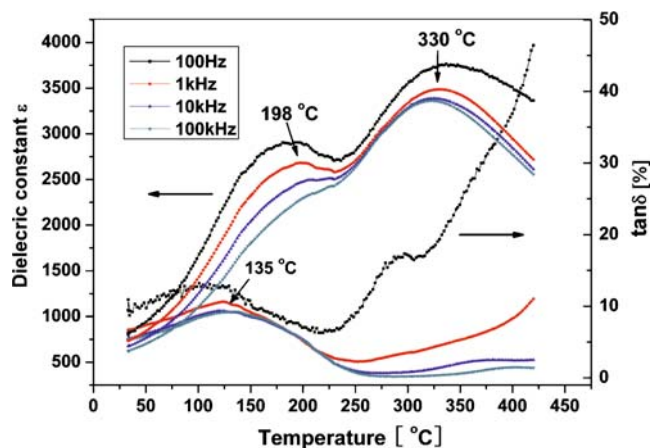


**Fig. 1** (color online) Temperature dependence of dielectric constant and loss in 0.94NBT-0.06BT crystals from 100 Hz to 1 MHz in the heating procedure

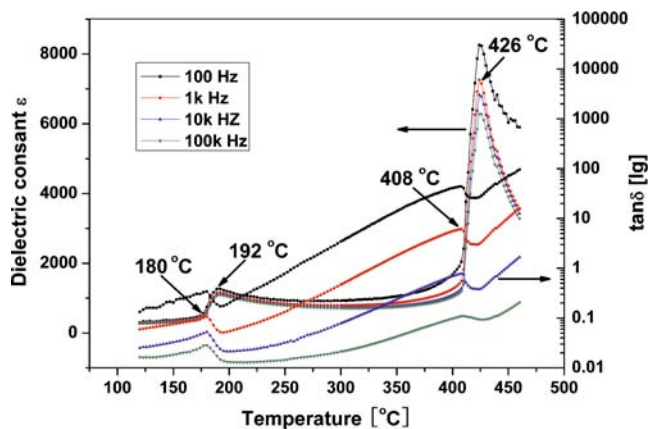


**Fig. 2** (color online) Temperature dependence of dielectric constant and loss in 0.95KNN-0.05LN crystals from 100 Hz to 1 MHz in the heating procedure

tetragonal phase transition at  $T_{ot} \sim 192^\circ\text{C}$  and ferroelectric tetragonal–paraelectric cubic phase transition at  $T_c \sim 426^\circ\text{C}$ . This  $T_c$  is lower than 0.96KNN-0.04LN and 0.94KNN-0.06LN ceramics [14], but is higher than that in the textured (K,Na)NbO<sub>3</sub>-based ceramics modified by adding Li, Ta and Sb [1]. For 0.95KNN-0.05LN crystals, the dielectric loss at 1 kHz rise slowly from 2.7% to 10.6% while the temperature goes up from 25°C to 180°C. From the comparison between NBBT and KNN–LN, it can be seen that the former has much broader phase transition peaks than the latter. However, the detailed phase transition process is not clear as yet.

### 3.2 In-situ observation of domain dynamics and phase transitions

The observation emphasis will be laid on NBBT crystals whereas detailed results of the KNN–LN system will be presented elsewhere.

0.94NBT-0.06BT sample only shows larger ferroelectric domain regions without sharp domain walls by the contrast of different interference color (Fig. 3(a)). The domain regions show clearer and clearer color stripe gradually with heating, and the change of domain configuration becomes accelerated while the sample is heated to 186–230°C (Fig. 3(b)). This rapid change of domains may be contributed to partly rhombohedral (R)-tetragonal (T) phase transition, in other words, R-phase and T-phase may coexist, predominated by the former, within this temperature range. The remarkable R–T phase transition takes place from 230°C to 240°C (Fig. 3(c)) and the T-phase is predominant in this temperature region. The antiferroelectric tetragonal phase shows domain stripes with gray interference color and different extinction

position from the rhombohedral phase (Fig. 3(d)). Therefore, both of R-phase and T-phase coexist within 54°C temperature range between 186°C–240°C, and R–T phase transition is diffusive, which is consistent with the broader dielectric peak near 198°C in the  $\epsilon$ – $T$  curve in Fig. 1.

It is seen that antiferroelectric tetragonal–paraelectric cubic (T–C) phase transition of 0.94NBT-0.06BT sample takes place at 255°C (Fig. 3(e)), which is 75°C lower than the  $T_m$  in the  $\epsilon$ – $T$  curve in Fig. 1. The C-phase is identified by the complete extinction. Moreover, it is surprising that the antiferroelectric T-phase (bright area) does not disappear and coexists with the paraelectric C-phase (dark area) at 535°C (Fig. 3(f)), and even at 700°C, which is much higher than its Curie temperature (330°C), and some of T-phase exists in the form of macrodomains. Not all of macrodomains change into microdomains when the sample is heated to above  $T_m$  or  $T_c$ .

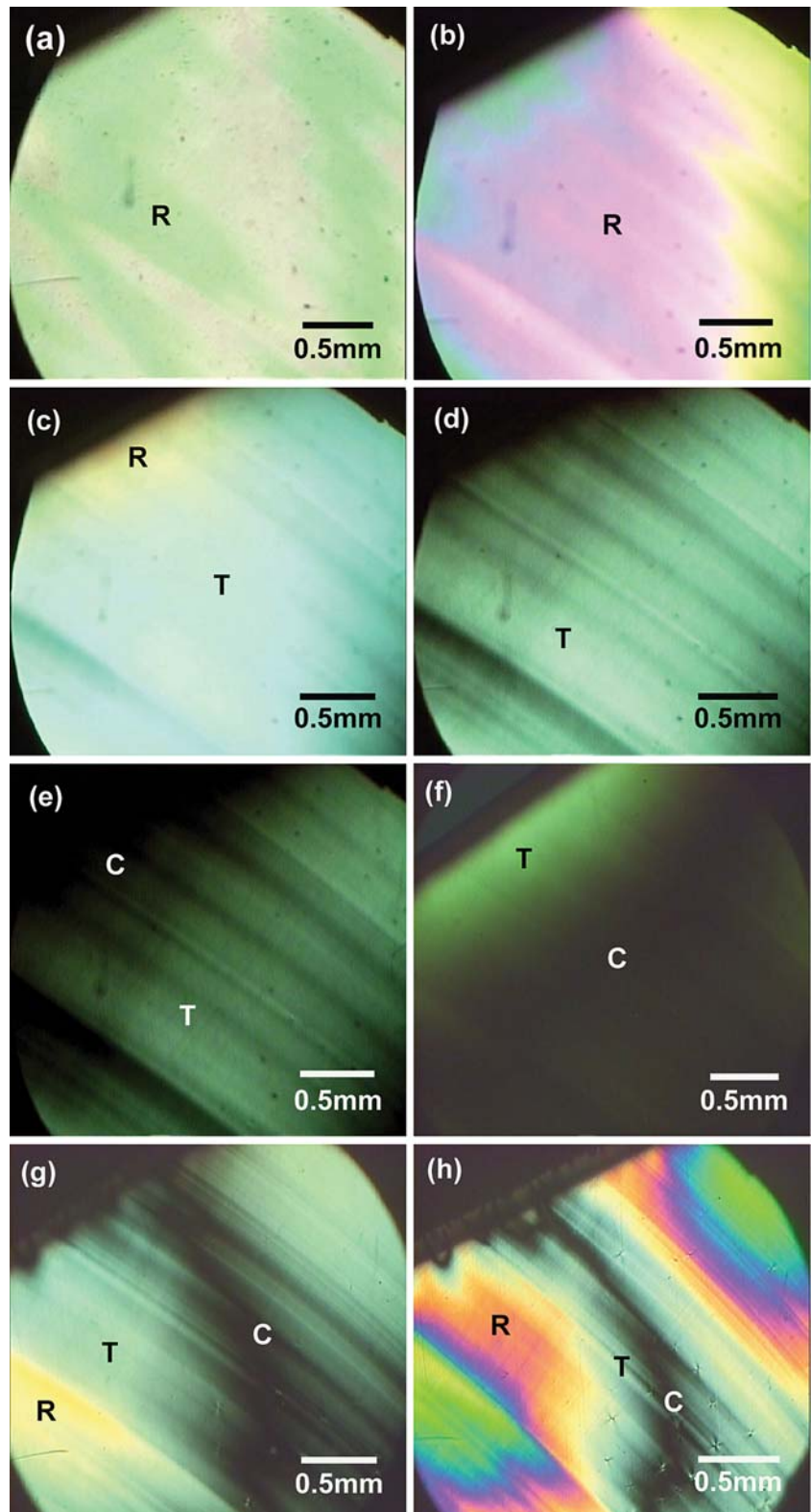
While the 0.94NBT-0.06BT sample undergoes successive cooling procedure from 700°C, it is seen that both of C-phase and T-phase coexist until 196°C and the new R-phase starts to appear at this temperature (Fig. 3(g)). After the sample is cooled to room temperature, domain configuration becomes stripes with clear domain walls, and R-phase is predominant, but T-phase, even C-phase exists in some regions (Fig. 3(h)). Domain configuration changes obviously after the sample experiences the heating and cooling procedure. The above observation demonstrates that the structure of 0.94NBT-0.06BT sample is sensitive to heating history. It is rational to assume that the lower value of  $d_{33}$  constant may originate from the remnant phases of high temperature antiferroelectric T-phase, even paraelectric C-phase in the matrix of low temperature ferroelectric R-phase besides the high coercive field  $E_c$  of NBT-based materials, which may enhance the difficulties in poling samples.

As for KNN–LN crystal, it is found that its phase transitions, both of O–T and T–C transformation, occur more abruptly than NBBT's. This suggests that KNN–LN is of more normal ferroelectrics whereas NBBT of more relaxor ferroelectrics. In addition, it is observed that like NBBT, T-phase does not disappear completely even at 600°C in KNN–LN sample.

## 4 Conclusions

NBBT and KNN–LN crystals have been grown by the Bridgman technique and excellent piezoelectric properties have been achieved in KNN–LN crystals. As for 0.94NBT-0.06BT crystals, domain dynamics and phase transition have been presented through in-situ observation. It is found that both of R–T and T–C phase transition are diffusive in NBBT and its structure is sensitive to the heating history. Its lower  $d_{33}$  constant may be related to the coexistence of antiferroelectric and ferroelectric phases at room temperature.

**Fig. 3** (color on line) In-situ observation results of domain dynamics and phase transition under a polarizing microscopy while heating and cooling 0.94NBT-0.06BT crystals. (a)–(f) are in heating procedure and (g), (h) in cooling one: (a) 25°C, (b) 210°C, (c) 238°C, (d) 248°C, (e) 255°C, (f) 535°C, (g) 196°C, (h) 25°C



**Acknowledgments** This work was supported by the space materials research project and 863 projects (No. 2008AA03Z411) in China.

## References

1. Y. Saito, H. Takao, T. Tani, T. Nonoyama, K. Takatori, T. Homma, T. Nagaya, M. Nakamura, *Nature* **432**, 84 (2004). doi:10.1038/nature03028
2. J.F. Carroll III, D.A. Payne, Y. Noguchi, M. Miyayama, Proceedings of International Symposium on the Application of Ferroelectrics (ISAF) in Nara, Japan in May, 2007
3. S.-E. Park, T.R. Shrout, *J. Appl. Phys.* **82**, 1804 (1997). doi:10.1063/1.365983
4. T. Kobayashi, S. Shimanuki, S. Saitoh, Y. Yamashita, *Jpn. J. Appl. Phys.* **36**, 6035 (1997). doi:10.1143/JJAP.36.6035
5. G. Xu, H. Luo, Y. Guo, Y. Gao, H. Xu, Z. Qi, W. Zhong, Z. Yin, *Solid State Commun.* **120**, 321 (2001). doi:10.1016/S0038-1098(01)00387-8
6. Y.M. Chiang, G.W. Farrey, A.N. Soukhojak, *Appl. Phys. Lett.* **73** (25), 3683 (1998). doi:10.1063/1.122862
7. G. Xu, Z. Duan, X. Wang, D. Yang, *J. Cryst. Growth* **275**, 113 (2005). doi:10.1016/j.jcrysgro.2004.10.074
8. K. Chen, G. Xu, D. Yang, X. Wang, J. Li, *J. Appl. Phys.* **101**, 044103 (2007). doi:10.1063/1.2562464
9. B.J. Chu, D.R. Chen, G.R. Li, Q.R. Yin, *J. Eur. Ceram. Soc.* **22**, 2115 (2002). doi:10.1016/S0955-2219(02)00027-4
10. Y. Hosono, K. Harada, Y. Yamashita, *Jpn. J. Appl. Phys.* **40**, 5722 (2001). doi:10.1143/JJAP.40.5722
11. X.J. Yin, H.C. Chen, W.W. Cao, M.L. Zhao, D.M. Yang, G.P. Ma, C.H. Yang, J.R. Han, *J. Cryst. Growth* **281**, 364 (2005). doi:10.1016/j.jcrysgro.2005.03.068
12. P. Zhao, B.-P. Zhang, *Appl. Phys. Lett.* **90**, 242909 (2007). doi:10.1063/1.2748088
13. T. Oh, M.-H. Kim, *Mater. Sci. Eng. B* **132**, 239 (2006). doi:10.1016/j.mseb.2006.02.070
14. Y. Guo, K. Ken-ichi, H. Ohsato, *Appl. Phys. Lett.* **85**, 4121 (2004). doi:10.1063/1.1813636